JMEPEG (2024) 33:7445–7453
https://doi.org/10.1007/s11665-024-09253-5

1059-9495/$19.00

ORIGINAL RESEARCH ARTICLE

Electrical, Mechanical, and Electromechanical Properties of Screen-Printed Piezoresistive Polydimethylsiloxane with Multiwalled Carbon Nanotube Nanocomposites

S. Riyaz Ali, A.L.G.N. Aditya, E. Megalai, R. Madhukaran, J. Kathirvelan, and E. Rufus

Submitted: 17 February 2023 / Revised: 6 October 2023 / Accepted: 23 January 2024 / Published online: 23 February 2024

Polydimethylsiloxane (PDMS) with multiwalled carbon nanotubes (MWCNT) fillers is a piezoresistive nanocomposite which is conformable, printable, and biocompatible. It is widely employed as a sensing layer in flexible pressure sensors, electronic skin (e-skin) of humanoid robots and as wearable sensors. Piezoresistive nanocomposites show significant increase in their electrical conductivity above a certain percolation threshold. In this work, PDMS + MWCNT-based sensing layers with different nanofiller MWCNT concentrations (2, 4 and 7 wt.%) are screen-printed and their electrical, mechanical, and percolation threshold responses are verified. The static I–V characteristics of the samples for a biasing DC voltage of 0-6 V are studied. The tensile test confirms maximum elongation of more than 50 mm. The change in resistance was minimal for 2 wt.% sample as the MWCNT's are sparsely distributed and no conducting channels are formed; for the 7 wt.% sensing layer, negligible change in resistance was observed as the conducting channels are broken. The highest change in resistance of 2.4 MΩ was observed after the percolation threshold value of 4 wt.% of the nanofiller concentration was reached. Overall, the 4 wt.% screen-printed piezoresistive nanocomposite layer showed highest sensitivity with a gauge factor of 4.76 and a linear response suitable for industrial applications.

Keywords flexible piezoresistive sensor, PDMS + MWCNT nanocomposite, percolation threshold, screen printing

1. Introduction

Physiological parameters of the human body such as body movement, temperature, bending angle and rotation of various body parts have been successfully measured by polymer-based flexible wearable sensors (Ref 1). Reasons for polymer-based sensors to grow in demand over highly accurate and fast IC-based silicon sensors are their conformability, ease in fabrication and low-cost in production (Ref 2). State-of-the-art flexible sensors can be fabricated by various techniques which include soft lithography (Ref 3), microcontact transfer printing (Ref 4), deep etching process (Ref 5), vacuum filtration (Ref 6), screen printing (Ref 7), etc. Screen-printing technique is widely used in the printing of flexible wearable sensors as it is a layer-by-layer approach of sensor design with an ability to print over a large area of the substrate in a single sweep. Other advantages of screen printing include, easily customizable sensor geometry, readily scale up/down sensor pattern, minimum material wastage and fabrication at ambient room temperature (Ref 7).

S. Riyaz Ali, A.L.G.N. Aditya, E. Megalai, R. Madhukaran, J. Kathirvelan, and **E. Rufus**, School of Electronics Engineering, Vellore Institute of Technology, Vellore, Tamil Nadu 632014, India. Contact e-mail: elizabethrufus@vit.ac.in.

In this work, a PDMS+MWCNT-based flexible piezoresistive nanocomposite sensor is screen-printed with different weight concentrations (wt.%) of MWCNT mixed in PDMS. Polymers like PVDF (Ref 8), polylactic acid (Ref 9), polyaniline (Ref 10) are also employed in the fabrication of conductive nanocomposites, and PDMS has been chosen for this work as it has multiple advantages over the aforesaid polymers. PDMS is chemically inert, transparent, highly flexible, and stable over wide temperature ranges. The commercial availability and biocompatibility of the pure PDMS whose tensile strength is 5.13 MPa makes it an excellent choice as an ink for screen printing (Ref 11). Nanomaterials are added as a reinforcement in polymers as they enhance the electrical, mechanical, and thermal properties of the composites. Broadly there are two different mechanisms for mixing CNT filler concentrations in the PDMS elastomer, namely dry blending method and wet mixing method.

1.1 Dry Blending Method

Preparation of PDMS + MWCNT using shear mixing and rotation mechanisms falls under the dry blending method. Here, the nanocomposites have higher tensile strength and thermal stability because of better nanotube dispersion in the elastomer (Ref 12). As no solvents are involved, it takes less curing time and it is a safe and non-toxic method as compared to wet mixing method (Ref 13). Shear mixing and rotation may physically damage the CNT and deform its shape resulting in shorter length and low aspect ratio. This forms a non-conductive path hampering their electrical conductivity and forming internal clusters of more than 10 μm size (Ref 14).

1.2 Wet mixing Method

To achieve uniform dispersion of CNT's in PDMS solution, initially the CNTs are suspended in an organic solvent and sonicated under a prescribed frequency and duration. PDMS elastomer is now added to this nanofilled solvent and sonicated. Lastly, PDMS curing agent is added and manually stirred. The conductive solution is then desiccated to remove the unwanted air pockets (Ref 15). Rheological properties of thus prepared solution are very important for screen-printing application. The wet mixing method enhances the electrical conductivity and electromechanical sensitivity of the nanocomposite, as herein the CNTs do not break in length when sonicated. The CNTs retain their high aspect ratio and uniform dispersion reduces the agglomeration of the internal clusters to 3 μm size.

Major considerations in the wet mixing method are that it takes longer time for curation and removal of entrapped air pockets from the solution (Ref 16). Also using non-polar solvents like toluene swell the PDMS matrix, whereas alcoholic solvents like methyl/ethyl alcohol have low affinity to CNT's surface because of their short hydrophobic region (Ref 17). Commonly used solvents like chloroform take less time for curation as they have a boiling temperature of 61.2 °C and show higher affinity to CNT's surface bonding with PDMS. The toxic and highly volatile nature of Chloroform should be mandatorily kept in mind and prescribed safe amounts of Chloroform should only be used for mixing. This work has been carried out using 99.5% pure AR-grade chloroform, stabilized with 1-2% *v/v* ethanol as the solvent for dispersing the CNT's in preparing the solutions to be used as ink in screen printing.

Most conventional methods (Ref 18, 19) use macromolds for fabricating sensing layers in the desired size and shape. Using macromolds produces sensors with a thick layer which reduces sensitivity of the sensor and requires more time for curing. Also, it is not possible to conveniently modify the mold shape or scale its size. A simpler, cost effective and faster approach for developing flexible sensory layers is by screen printing technique. Generally, screen-printed sensors have a thickness of 30-40 microns and thereby deliver highly sensitive sensory layers (Ref 20). Table 1 shows applications of screen-printed PDMS + MWCNT sensory layers reported in the literature in diverse fields of industrial pressure sensors, humanoid robot E-skin, wearable electronics, and biomedical applications.

As evident from Table 1, electrical, mechanical, and temperature-based characterizations of piezoresistive nanocomposites have been mostly reported. Percolation law behavior perspective of nanocomposites has not been focused in the literature. Novelty of this work is in demonstrating the percolation law response of the piezoresistive nanocomposites, which is an important consideration for the electromechanical response of PDMS + MWCNT based nanocomposites. Response of the nanocomposite sensory layer depends on the CNT filler size, shape and concentration added in the polymer matrix. Nanocomposites behave as an insulator at lower filler concentrations (typically 0.5-1.5 wt.%) and are electrically saturated at higher filler concentrations (typically $>$ 6 wt.%). Nanocomposites show highest sensitivity and change in resistance at intermediate filler concentrations after crossing a percolation threshold value (typically 3-4 wt.%) (Ref 30). Sensory layers should be screen-printed by preparing sample inks with nanofiller concentration having optimal sensitivity

Table 1 Applications and characterization of screen-printed sensory layers

Year	Sensory layer	Application	Characterization reported	Reference
2010	PDMS + MWCNT	Strain measurement in microstructures	Change in resistance for mechanical deformations	Ref 21
2015	PDMS + CNT	Pressure sensors for Robotic E-skin	Change in resistance for normal pressure applied	Ref 22
2015	PDMS + MWCNT	Plantar pressure monitoring in Ulcer prevention	Mechanical properties axial and normal force	Ref 23
2015	PDMS + MWCNT(Electrode)/Silver flake ink on flexible PET substrate	Dry electrode for ECG measurements	ECG signal electrical output	Ref 24
2017	PDMS + CNT	Capacitive pressure sensor	Change in capacitance for varying pressures	Ref 25
2019	Graphite flakes/PDMS + MWCNT	Flexible temperature sensor	Rheological behavior/Thermal gravimetric analysis	Ref 26
2020	PDMS + CNT	Flexible resistive temperature detector (RTD)	Change in resistance subject to different temperature ranges	Ref 27
2022	PDMS + MWCNT	Omnidirectional strain sensor for wearable electronics	Rheological behavior for shear stress and strain cyclic tests	Ref 28
2022	PDMS + CNT	Detection of multiple avian influenza virus antigens	Electrochemical analysis	Ref 29

response. Here, percolation behavior of PDMS+MWCNT sensory layers with 2, 4 and 7 wt.% concentrations is considered. This analysis would be useful in determining nanofiller concentrations for screen-printing sensory layers. Preparation of sample ink with 2%, 4% and 7% weight of MWCNT in PDMS solution has been discussed in section 2. Electrical, mechanical, and electromechanical responses of the 3 sensing layers printed using screen-printing technique are discussed in the results section.

2. Preparation of Screen-Printing Materials

The layer thickness of the screen-printed PDMS+MWCNT sensor is only around 100 microns, and therefore, tears apart easily while peeling-off the substrate after curing. Also, such a thin layer becomes vulnerable to permanent physical damage when grippers are clamped to the sample for mechanical and electrical properties measurement.

To overcome these issues, we have used the mesh for screen printing with a smaller number of TPI (threads per inch), that is 120 TPI to be specific, for all our samples. Wider gaps make the mesh porous and maximum ink penetrates through the mesh and deposits on the substrate. Secondly, the manual squeegee was swept multiple times over the mesh, until all the ink has been passed down through the stencil of the mesh. Finally, the mesh has been deliberately raised 5 mm above the substrate to give an embossed type of printing on the substrate and henceforth increase layer thickness. By implementing these steps, we have successfully printed mechanically rugged flexible PDMS + MWCNT sensors with 3 different weight ratios and having physical dimensions of 80 × 15 × 1 mm.

Table 2 Volume fractions of components used in ink preparation

			PDMS, ml	
wt.%	Chloroform, ml	MWCNT, gms	Part-A	Part-B
2 wt.%	20	0.3	15	3
4 wt.%	20	0.7	15	3
7 wt.%	30	1.2	15	3

For dispersion of MWCNT, ethanol stabilized organic solvent chloroform (trichloromethane, SRL Chemicals) with 99.5% purity is used. The MWCNT (Nano Research labs, India) has a diameter of 5-10 nm and volume resistivity of 0.1 Ω cm in a dry powder state. PDMS is standard SYLGARD-184 Silicone elastomer (Kevin Electrochem, India). The ultrasonic probe sonicator (DP-500, Dakshin Processors, India) employed is a powerful 500-watt equipment with 20 KHz maximum frequency. Samples are cured in hot furnace (Indfurr Industrial equipments, India) having heating capacity up to 200 °C.

The step-by-step process involved in preparation of ink is discussed clearly here, and the quantity of volume fraction of each compound used in the preparation of all 3 samples is listed in Table 2. Initially, MWCNT powder is mixed in chloroform and kept under probe sonicator for 15 mins with 10 seconds ON time and 5 seconds OFF time at 60 W power. Next, the sample is mixed with PDMS elastomer (Part-A) and again placed under the probe sonicator for a total of 60 mins with a frequency of 15 seconds ON time and 8 seconds OFF time. After the solution is properly mixed, PDMS curing agent (Part-B) is added in 1:5 proportion of Part A to the solution and manually stirred using a glass rod for 5 mins. Now the sample is placed inside a desiccator under a controlled environment to remove the unwanted bubbles.

After the sample is run through the desiccator, it is now poured onto the wooden frame, which has a 120 TPI silk fabric mesh stretched over it. Figure 1 depicts schematic representation of the operating set-up of the screen-printing process. Real-time setup of the screen-printing equipment along with a rectangular shaped stencil of 80 × 15 mm size, which is readily exposed on the same mesh is shown in the inset of Figure 1. The mesh frame is fixed at a height of 5 mm above the printing substrate to get thicker sensing layers. A 2-inch squeegee is used to sweep the ink manually through the rectangular opening onto a polyimide substrate.

The squeegee is run multiple times back and forth over the mesh until all the ink has passed onto the substrate. Now, the mesh with the rectangular shaped sensing layer printed on it is placed in a hot furnace at 100 °C for 20 mins for curing. After curing, the samples of size 80 × 15 mm are carefully peeled from the polyimide substrate. After peeling off, thickness of 2

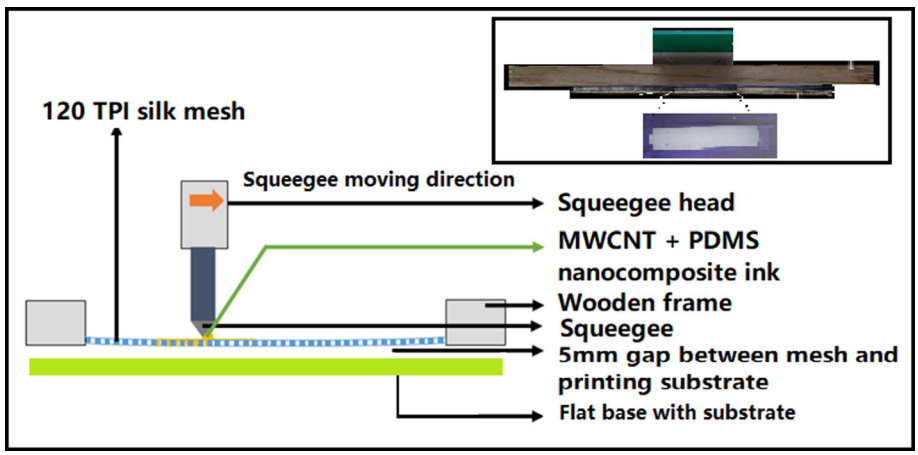

Figure 1 Schematic of screen-printing setup. Real-time apparatus along with readily exposed rectangular shape stencil on the mesh (Inset)

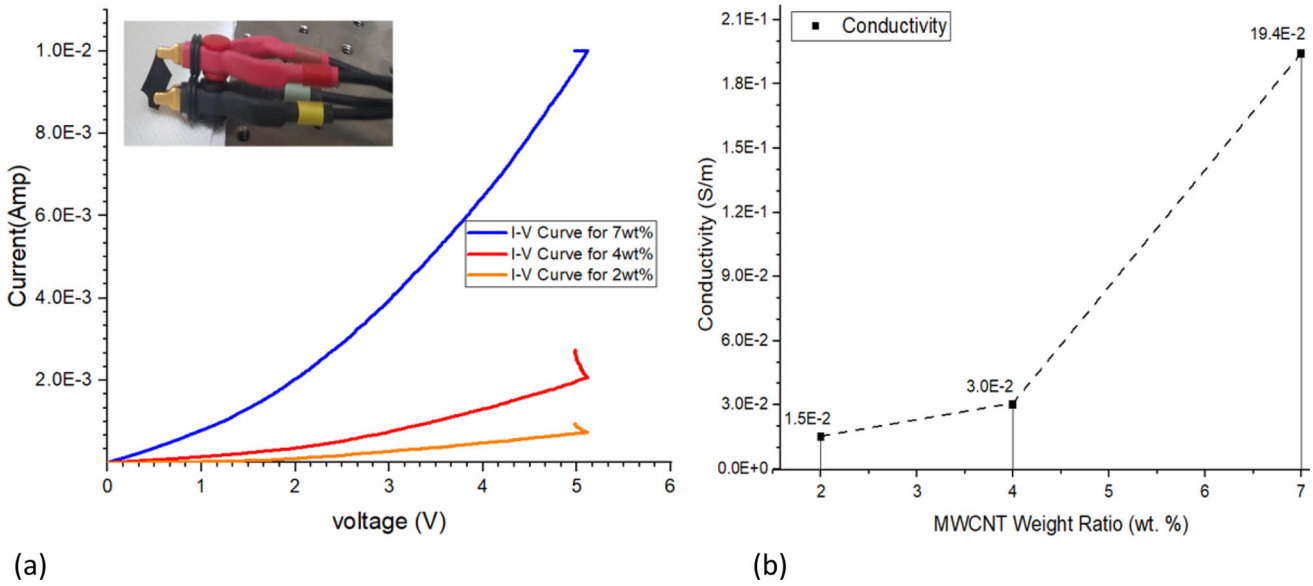

Figure 2 (a) I–V characteristics of 2, 4 and 7 wt.% Samples. Inset: Specialized soft grippers to hold the samples 2(b) Conductivity of screen-printed PDMS + MWCNT nanocomposites with 2, 4 and 7 wt.% ratios

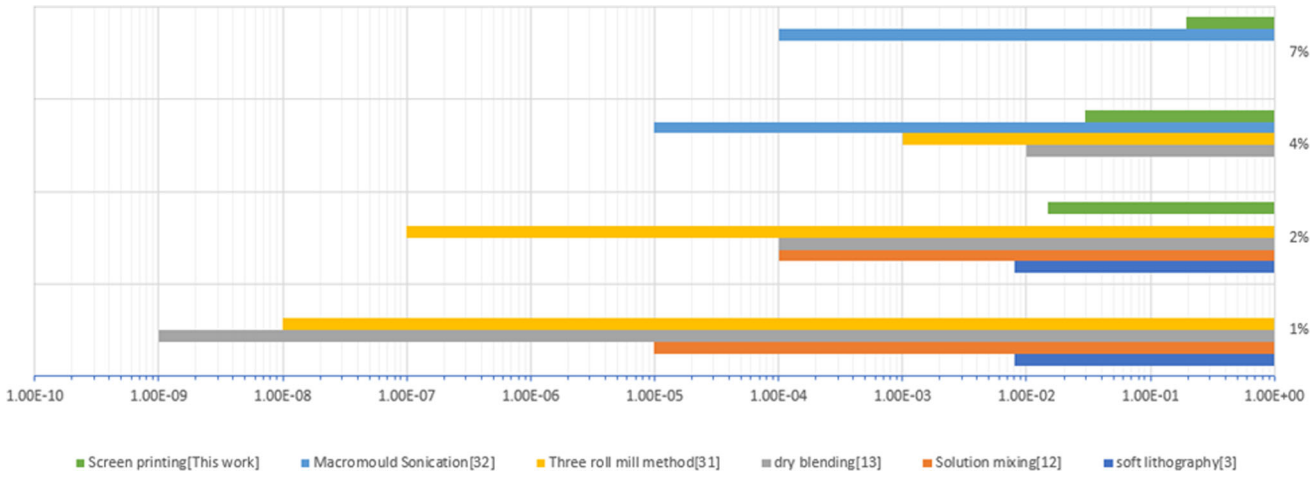

Figure 3 Comparison of electrical characterization of PDMS + MWCNT nanocomposites using different fabrication techniques

and 4 wt.% sensing layers is measured to be 0.75 mm, whereas the 7 wt.% sensing layer was thicker with 1 mm thickness.

3. Characterization and Discussion

All 3 samples of different compositions are subjected to electrical conductivity response using a precision I–V (current–voltage) measuring unit (Model-B2902B, Keysight technologies, India). The mechanical response is characterized using the tensile testing machine (Model-HKS50, Tinius Olsen, UK) and the piezoresistive response is measured by interfacing the tensile testing machine with a 6½ Digit Multimeter (DMM) (Model—34461A, Keysight technologies, India). Field Emission Scanning Electron Microscope (FESEM) characterization is done for all 3 samples using a sophisticated FESEM machine with an operative voltage of 10 KV (Model-Quanta FEG 250, Oxford Instruments, UK)

3.1 Electrical Characterization of the samples

Figure 2(a) shows the I–V characteristics of the 3 samples of 10 × 10 mm^2 size. Measurements are taken by holding them with specialized soft gripper electrodes of the I–V precision measurement device as shown in inset of Figure 2(a). The samples are biased over a voltage range of 0-6 V, and corresponding current passing through the sample is recorded at 0.1 KHz frequency. The 7 wt.% sample recorded the highest current conduction of 10 mA at 5 V supply.

Selection of a particular nanocomposite filler concentration for any application depends upon the conductivity, flexibility, and maximum operating range of the sensor. Sensor properties are engineered by altering the composites with fillers and binders independently or cohesively. The conductivity (S/m) of the screen-printed nanocomposites with different weight ratios was measured and the 7 wt.% sample was measured to be highest at 19.4e−2, whereas the 4 and 2 wt.% samples showed 3e−2 and 1.5e−2 conductivity, respectively, as shown in

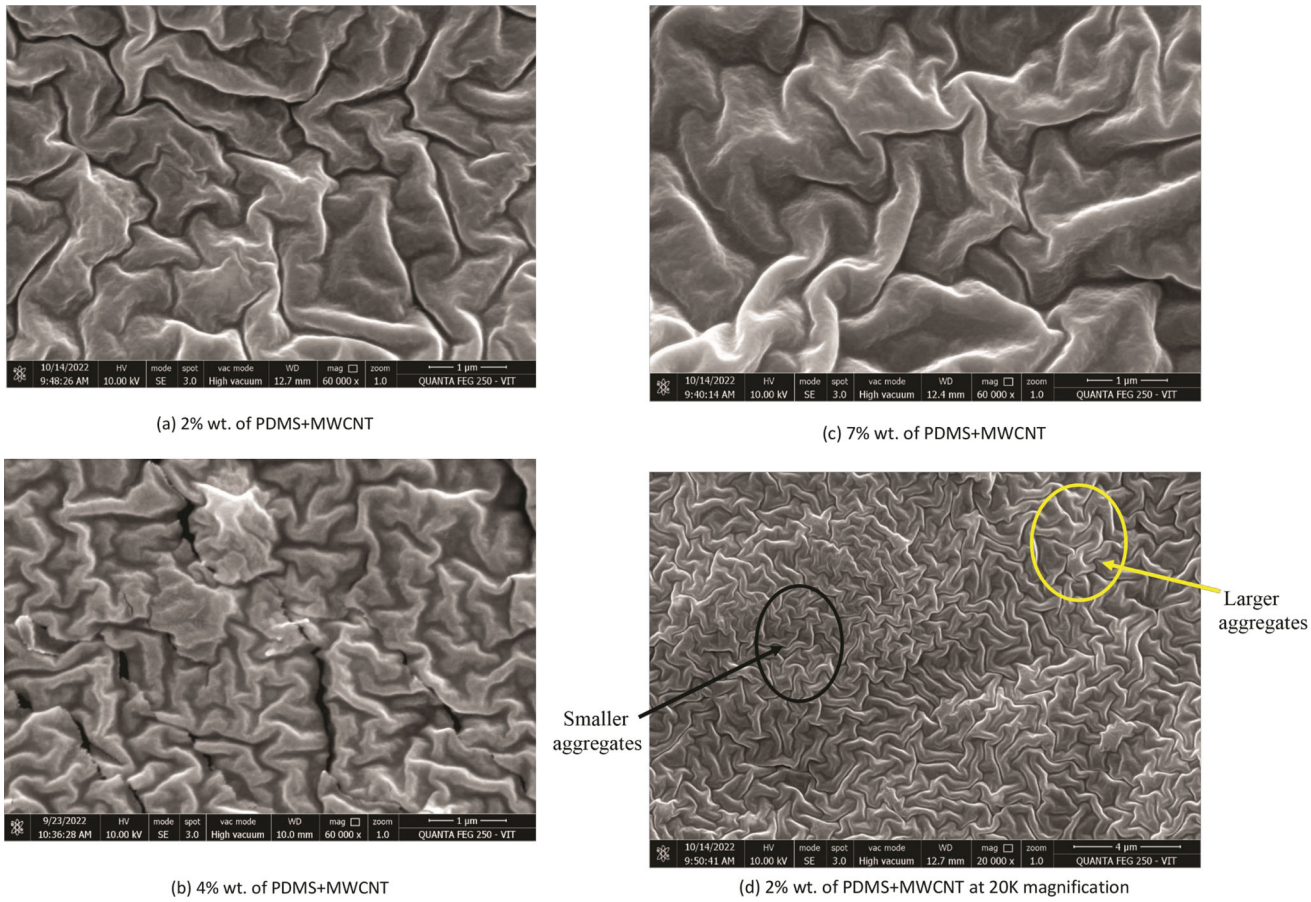

Figure 4 FESEM results for 2, 4 and 7 wt.% of screen-printed PDMS + MWCNT nanocomposites. (a) 2 wt.% of PDMS + MWCNT. (b) 4 wt.% of PDMS + MWCNT. (c) 7 wt.% of PDMS + MWCNT. (d) 2 wt.% of PDMS + MWCNT at 20 K magnification

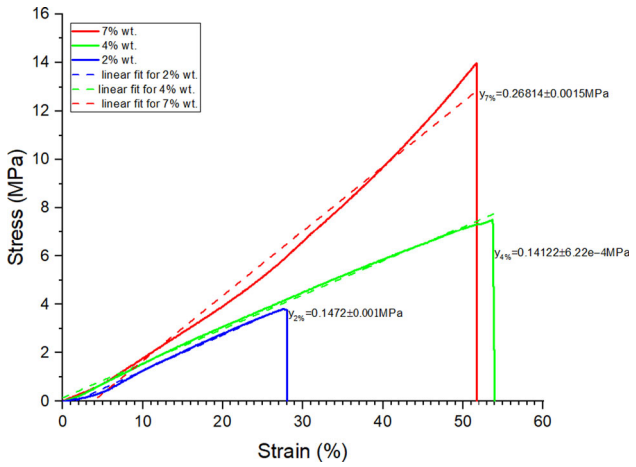

Figure 5 Stress–strain curve for tensile force response of the screen-printed nanocomposites

Figure 2(b). Figure 3 shows comparison of electrical conductivity of the PDMS+MWCNT nanocomposites fabricated with different techniques with present work.

The comparison shown in Figure 3 showcases the magnitude of conductivity achieved by different fabrication methods, herein direct comparison of electrical conductivity of the samples is not justified, as the samples reported in the literature differ in physical dimensions and thickness. However, the electrical conductivity(S/m) of the 7 wt.% sample prepared by dry blending method is reported to be highest with 10e−1 S/m, produced better results than its screen-printed counterpart which is 19.4e−2 S/m. However, the dry blended sensor width is almost 30 times greater than the screen-printed sensor.

Increasing the filler concentration reduces the percolation threshold, but a major challenge is to overcome agglomeration of the MWCNT at higher filler concentrations, as inter spacing between the CNT's reduces and van der Waals forces highly entangle with adjacent CNT. Therefore, study of internal arrangement of the PDMS+MWCNT nanocomposites is essential in determining the agglomerate formation which can be observed in the FESEM images shown in Figure 4(a-c). The images are captured over a 1 μm area with 60 k magnification. Figure 4(c) corresponding to 7 wt.% having the highest filler concentration of MWCNT has larger agglomerates, whereas the agglomeration reduces as the filler concentration decreases in 2 and 4 wt.% samples as shown in Figure 4(a) and (b), respectively. On the other hand, sparse distribution of MWCNT's in 2 wt.% results in very high initial resistance and limiting conductivity of the sample. Overall, sensor performance can only be estimated with the inclusion of all these parameters, wherein some key parameters like agglomeration leading to non-uniform deposition and viscosity of the ink have a major impact on the sensor performance even before the sensor is printed.

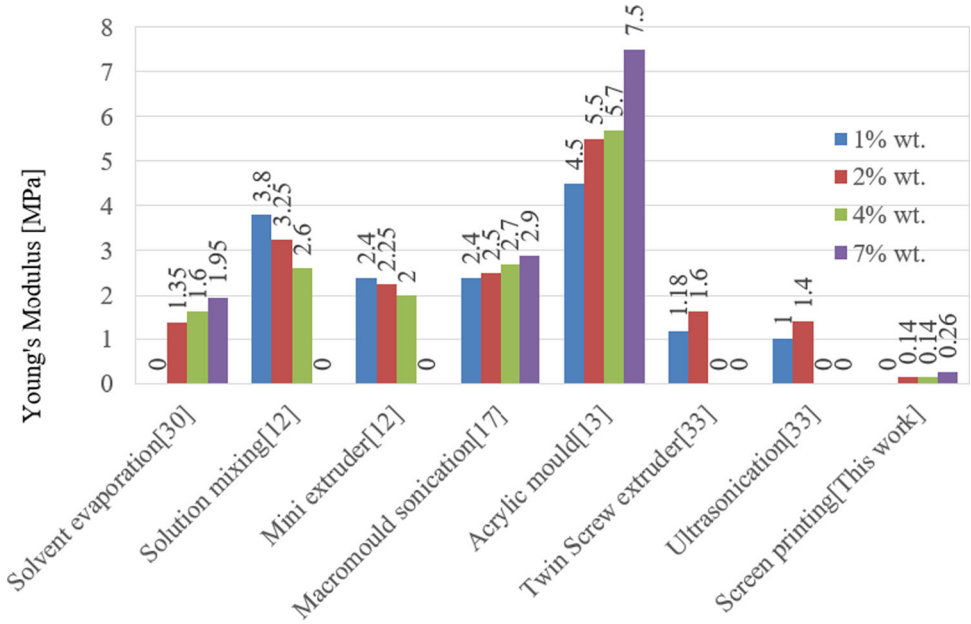

Figure 6 Comparison of mechanical characterization of PDMS + MWCNT nanocomposites using different fabrication techniques

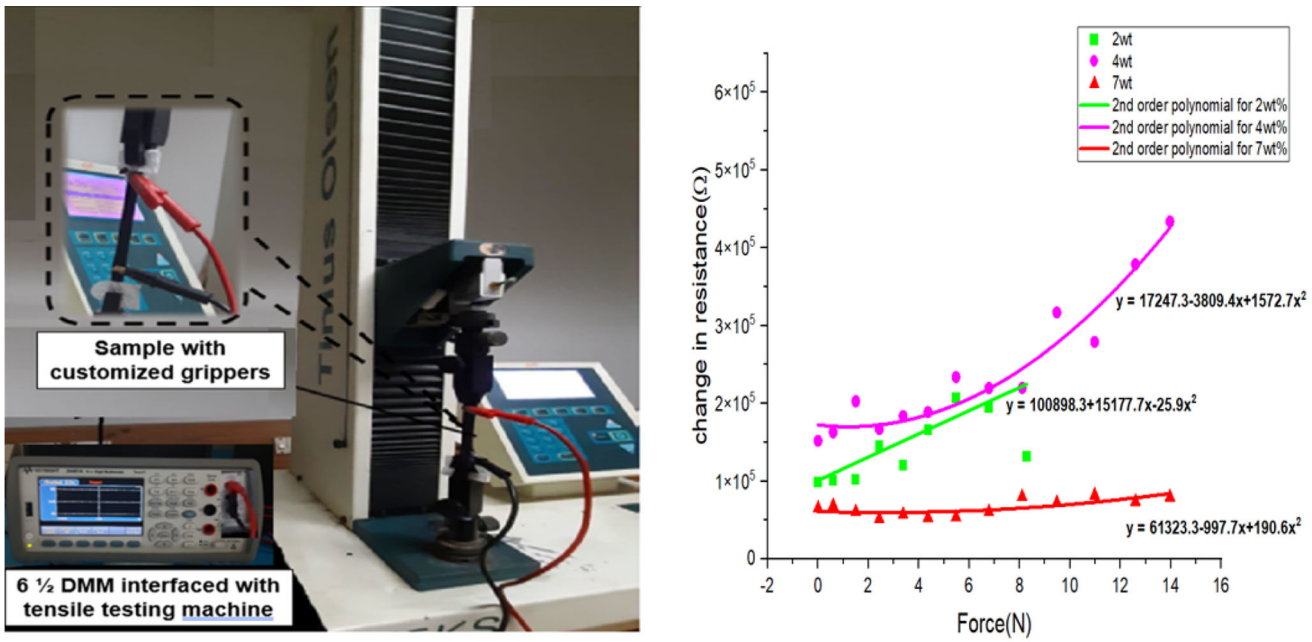

Figure 7 (a) Electromechanical response experimental setup. Customized grippers with electrodes (inset). (b) Second-order polynomial trendline of electromechanical response of the screen-printed nanocomposites

Visual comparison of Figure 4(a) and (b) reveals that the 2 wt.% sample forms larger aggregates than the 4% sample, which is not expected. The screen-printed polymer nanocomposites prepared from the conventional blending or sonication process may at times result in a random distribution of the fillers with non-uniform aggregation within the layer (Ref 34). This non-uniform distribution of nanofillers is more probabilistic in conventional blending process at lower concentrations of the nanofiller (0-2 wt.%), as dispensing of the MWCNT in the chloroform volume during sonication may be non-uniform at such lower concentrations of the filler (Ref 35). Figure 4d shows a 20 k magnification FESEM image of the same 2 wt.% sample, where non-uniform distribution of the nanofillers in the sample can be seen. For instance, the yellow circle on the top-right corner of the sample shows larger aggregates, whereas the black circle shows smaller aggregates, a non-uniform distribution within the same layer when a larger area is considered. Therefore, the 2 wt.% sample FESEM image

in Figure 4(a) in some areas can form denser aggregation than its 4 wt.% counterpart, but their electromechanical behavior is subject to percolation law of piezoresistive nanocomposites as shown in section 4.2.

3.2 Mechanical Characterization of the samples

The mechanical strength of the sensing layers is determined by loading the samples onto the grippers of the tensile testing machine and a step uniaxial tensile force of 0.2 N is applied on it. The maximum load range is set to 50 N, and the extension speed is set to 5 mm/min pace. The resultant plot is shown in Figure 5.

The physical elongation of 2 and 4 wt.% has shown a linear displacement with almost the same slope. The 2 wt.% sample being the most fragile of the 3 samples encountered necking at 28 mm, whereas the 4 wt.% showed necking effect at 55 mm. The thickness of the 7 wt.% sample being the highest showed a more plastic behavior with highest endurance up to 14 N while being stretched for 52 mm before necking. Overall, the 4 wt. sample showed both a linear and wider range of extension. Figure 6 shows comparative study of the highest elastic modulus of PDMS + MWCNT nanocomposite samples prepared using different fabrication techniques.

The mechanical rugged strength of PDMS+MWCNT screen-printed sensing layers is very less in comparison with macromold-based sensing layers. The Young's modulus of screen-printed layers showed a maximum of 0.26 MPa for 7 wt.% for 1 mm thick sample, whereas an acrylic mold fabricated 7 wt.%. sensing layer of 30 mm thickness was reported to be 7.5 MPa in (Ref 13). Mold-based thick samples can be highly repeatable sensor layers and physically rugged, but their sensitivity also decreases. Screen-printed layers are highly sensitive and conformable layers whose mechanical strength can further be improved using appropriate binders in the ink.

3.3 Electromechanical response of the samples

Conductivity in a nanocomposite sample depends mainly on two factors, CNT filler concentration and establishment of conductive paths within the sample. Filler concentration is not only a very critical factor, for observing changes in the resistance of the sample but also in ink preparation of screen-printing process. At low filler concentrations of MWCNT, the ink has low viscosity and disperses uncontrollably after printing on the substrate and therefore invades unwanted areas on the design layout. On the other hand, at higher filler concentrations, the ink agglomerates faster as the inter-spacing gap between MWCNT's reduces, resulting in non-uniform distribution of the ink on the printed substrate.

To analyze the change in resistance, all 3 specimens are cut in dog bone shape as per the ASTM D412 standards for tensile stress–strain properties of elastomers and loaded onto the tensile testing machine, where they are subjected to a tensile force varying from 0 to 16 N. The corresponding change in resistance is measured using a 6 $^{1}/_{2}$ DMM as shown in Figure 7(a). Customized grippers are used to firmly hold the sample without causing any damage, when an external force is applied. Corresponding change in resistance recorded for the 3 different filler concentrations are then plotted as shown in Figure 7(b). Percolation threshold for nanocomposites is achieved at intermediate filler concentrations; therefore, the sample with 4 wt.% showed the highest change in resistance varying from initial resistance of 0.15 MΩ to a final resistance of 0.58 MΩ at necking.

The overall change in resistance is 0.43 MΩ for 4 wt.% sample. The overall change in resistance for 2 wt.% sample is 0.15 MΩ, which is much less than 4 wt.% sample as the nanofiller content of MWCNT is lesser in 2 wt.% sample. Even though current conducting capacity of 7 wt.% sample is highest amongst the three samples, its change in resistance when subjected to mechanical deformation is least with overall change in resistance of 0.02 MΩ, because of the reorientation and eventual breakup of continuous conducting channels inside the nanocomposite layer.

At low filler concentrations, the initial offset resistances are very high and decrease gradually as filler concentrations increase. Higher filler concentrations offer least initial resistance, as shown in the plot of Figure 7(b) where the 7 wt.% sample offered the least initial offset resistance of 0.6 MΩ. Ideally, the 2 wt.% sample is expected to show highest initial resistance than the 4 wt.% sample, but we have recorded the 4 wt.% sample having 0.5 MΩ higher offset resistance than the 2 wt.% sample. Persistent conducting paths in the 2 wt.% sample or non-uniform distribution of nanofiller could be a reason causing this abnormality. The second order polynomial curve fitting used to represent the data points for the 3 samples, aid to visualize the sensor behavior in response to normal force. The 2 and 7 wt.% sample response data points are less divergent and can also be linear fitted as they have shown short range of change in resistance. But the 4 wt.% sample response requires second order polynomial curve fitting, as the data points recorded are spread over a wide range of 0.43 MΩ of change in resistance in a nonlinear fashion along the applied 0-14 N normal force. The second order curve fitting for 4 wt.% sample shows the lower operating range (0-4 N) has minimal change in resistance of only 0.1 MΩ and above 4 N there is a surge in the change resistance of nearly 2.4 MΩ as the force is increased up to 14 N adhering to percolation law of conducting nanocomposites.

4. Conclusion

Flexible polymer nanocomposite-based piezoresistive sensors of 2%, 4% and 7 wt.% volume fractions of MWCNT have been successfully fabricated using screen printing, and their electrical, mechanical, and electromechanical responses have been verified. The desired properties of the sensors are engineered by altering the composite with fillers and binders independently or cohesively, despite the resistivity of the device depends upon the dimensions and percolation threshold. So, the major objective of this paper is studying the percolation mechanism of different concentrations of nanocomposite (PDMS + MWCNT). The one major challenge of these composites is with the fillers which are immiscible, which leads to agglomerates at high concentration of them. This leads to inconsistent print of the sensor and greater scalability of the conductivity with 1D to 2D and 3D structures (with respect to thickness) which is observed in 7 wt.% where controlling the thickness is a challenging objective. Overall, PDMS + MWCNT-based piezoresistive sensors with 4 wt.% resulted in the highest change in resistance, having a linear response over a wider operating range of up to 14 N. Mechanical

durability and tensile strength are good in 7 wt.% sample. Although screen-printing technique in general is a promising fabrication technique with high customization, scalability and repeatability with the above-mentioned constraints, variations in conductivity are evident. So, estimating this variation is crucial in determining the performance and resolution of the devices. In future, a matrix grid of piezoresistive sensors can be screen-printed with a lesser TPI-Mesh and its electromechanical response with repeatability can be verified over a large-area flexible pressure sensors in diversified applications.

References

1. S.C. Mukhopadhyay, N.K. Suryadevara, and A. Nag, Wearable Sensors for Healthcare: Fabrication to Application, *Sensors*, 2022, **22**(14), p 5137.
2. F. Schneider, J. Draheim, R. Kamberger, and U. Wallrabe, Process and Material Properties of Polydimethylsiloxane (PDMS) for Optical MEMS, *Sens. Actuators A*, 2009, **151**(2), p 95-99.
3. A. Khosla and B.L. Gray, Preparation, Characterization and Micromolding of Multi-walled Carbon Nanotube Polydimethylsiloxane Conducting Nanocomposite Polymer, *Mater. Lett.*, 2009, **63**(13-14), p 1203-1206.
4. S. Hassan, M.S. Yusof, S. Ding, M.I. Maksud, M.N. Nodin, K.A. Mamat, M.S. Sazali, and M.Z. Rahim, Investigation of Carbon Nanotube Ink with PDMS Printing Plate on Fine Solid Lines Printed by Micro-flexographic Printing Method, in IOP Conference Series: Materials Science and Engineering, vol. 203, no. 1 (2017), p. 012017, IOP Publishing
5. L. Yu, C. Shearer, and J. Shapter, Recent Development of Carbon Nanotube Transparent Conductive Films, *Chem. Rev.*, 2016, **116**(22), p 13413-13453.
6. X. Wang, G. Li, R. Liu, H. Ding, and T. Zhang, Reproducible Layer-by-Layer Exfoliation for Free-Standing Ultrathin Films of Single-Walled Carbon Nanotubes, *J. Mater. Chem.*, 2012, **22**(41), p 21824-21827.
7. J. Machiels, A. Verma, R. Appeltans, M. Buntinx, E. Ferraris, and W. Deferme, Printed Electronics (PE) as an Enabling Technology to Realize Flexible Mass Customized Smart Applications, *Procedia CIRP*, 2021, **96**, p 115-120.
8. J.K. Wang, G.M. Xiong, M. Zhu, B. Özyilmaz, A.H. Castro Neto, N.S. Tan, and C. Choong, Polymer-Enriched 3D Graphene Foams for Biomedical Applications, *ACS Appl. Mater. Interfaces*, 2015, **7**(15), p 8275-8283.
9. G. Kaur, R. Adhikari, P. Cass, M. Bown, and P. Gunatillake, Electrically Conductive Polymers and Composites for Biomedical Applications, *RSC Adv.*, 2015, **5**(47), p 37553-37567.
10. S.B. Park, E. Lih, K.S. Park, Y.K. Joung, and D.K. Han, Biopolymer-Based Functional Composites for Medical Applications, *Prog. Polym. Sci.*, 2017, **68**, p 77-105.
11. R. Ariati, F. Sales, A. Souza, R.A. Lima, and J. Ribeiro, Polydimethylsiloxane Composites Characterization and its Applications: A Review, *Polymers*, 2021, **13**(23), p 4258.
12. K.T.S. Kong, M. Mariatti, A.A. Rashid, and J.J.C. Busfield, Effect of Processing Methods and Functional Groups on the Properties of Multi-Walled Carbon Nanotube Filled Poly (dimethyl siloxane) Composites, *Polym. Bull.*, 2012, **69**(8), p 937-953.
13. J. Du, L. Wang, Y. Shi, F. Zhang, S. Hu, P. Liu, A. Li, and J. Chen, Optimized CNT-PDMS Flexible Composite for Attachable Health-Care Device, *Sensors*, 2020, **20**(16), p 4523.
14. W. Bin, M.M. Hossain, and S.H. Kong, PDMS-based Two-Axis Inclinometer with a 360-Degree Measuring Range, *Sens. Actuators A*, 2016, **239**, p 54-60.
15. N. Hu, H. Fukunaga, S. Atobe, Y. Liu, and J. Li, Piezoresistive Strain Sensors Made from Carbon Nanotubes-Based Polymer Nanocomposites, *Sensors*, 2011, **11**(11), p 10691-10723.
16. J. Hwang, J. Jang, K. Hong, K.N. Kim, J.H. Han, K. Shin, and C.E. Park, Poly (3-hexylthiophene) Wrapped Carbon Nanotube/poly (dimethyl siloxane) Composites for Use in Finger-Sensing Piezoresistive Pressure Sensors, *Carbon*, 2011, **49**(1), p 106-110.
17. J.H. Kim, J.Y. Hwang, H.R. Hwang, H.S. Kim, J.H. Lee, J.W. Seo, U.S. Shin, and S.H. Lee, Simple and Cost-Effective Method of Highly Conductive and Elastic Carbon Nanotube/Polydimethylsiloxane Composite for Wearable Electronics, *Sci. Rep.*, 2018, **8**(1), p 1-11.
18. N. Sankar, M.N. Reddy, and R.K. Prasad, Carbon nanotubes Dispersed Polymer Nanocomposites: Mechanical, Electrical, Thermal Properties and Surface Morphology, *Bull. Mater. Sci.*, 2016, **39**(1), p 47-55.
19. P. Ghahramani, K. Behdinan, R. Moradi-Dastjerdi, and H.E. Naguib, Theoretical and Experimental Investigation of MWCNT Dispersion Effect on the Elastic Modulus of Flexible PDMS/MWCNT Nanocomposites, *Nanotechnol. Rev.*, 2022, **11**(1), p 55-64.
20. Web Article: https://www.rheologylab.com/articles/coatings-paints-inks/screen-printing-ink-paste/
21. C.-X. Liu and J.-W. Choi, Strain-Dependent Resistance of PDMS and Carbon Nanotubes Composite Microstructures, *IEEE Trans. Nanotechnol.*, 2010, **9**(5), p 590-595. https://doi.org/10.1109/TNANO.2010.2060350
22. N. Yogeswaran, S. Tinku, S. Khan, L. Lorenzelli, V. Vinciguerra, and R. Dahiya, Stretchable Resistive Pressure Sensor Based on CNT-PDMS Nanocomposites, in 2015 11th Conference on Ph.D. Research in Microelectronics and Electronics (PRIME), Glasgow, (2015) pp. 326-329, https://doi.org/10.1109/PRIME.2015.7251401
23. C. Gerlach et al., Printed MWCNT-PDMS-Composite Pressure Sensor System for Plantar Pressure Monitoring in Ulcer Prevention, *IEEE Sens. J.*, 2015, **15**(7), p 3647-3656. https://doi.org/10.1109/JSEN.2015.2392084
24. A.A. Chlaihawi, B.B. Narakathu, A. Eshkeiti, S. Emamian, S.G.R. Avuthu, and M.Z. Atashbar, Screen Printed MWCNT/PDMS Based Dry Electrode Sensor for Electrocardiogram (ECG) Measurements, in 2015 IEEE International Conference on Electro/Information Technology (EIT), Dekalb, (2015), pp. 526-529, https://doi.org/10.1109/EIT.2015.7293392
25. D. Maddipatla, B.B. Narakathu, M.M. Ali, A.A. Chlaihawi, and M.Z. Atashbar, Development of a Novel Carbon Nanotube Based Printed and Flexible Pressure Sensor, in 2017 IEEE Sensors Applications Symposium (SAS), Glassboro, (2017) pp. 1-4, https://doi.org/10.1109/SAS.2017.7894034
26. L. Wu, J. Qian, J. Peng et al., Screen-printed Flexible Temperature Sensor Based on FG/CNT/PDMS Composite with Constant TCR, *J. Mater. Sci. Mater. Electron.*, 2019, **30**, p 9593-9601. https://doi.org/10.1007/s10854-019-01293-1
27. X. Zhang, D. Maddipatla, A.K. Bose, B.B. Narakathu, and M.Z. Atashbar, A Printed MWCNTs/PDMS Based Flexible Resistive Temperature Detector, in 2020 IEEE International Conference on Electro Information Technology (EIT), Chicago, (2020), pp. 509-513, https://doi.org/10.1109/EIT48999.2020.9208334
28. Y. Yang, H. Wang, Y. Hou, S. Nan, Y. Di, Y. Dai, F. Li, and J. Zhang, MWCNTs/PDMS Composite Enabled Printed Flexible Omnidirectional Strain Sensors for Wearable Electronics, *Compos. Sci. Technol.*, 2022, **28**(226), p 109518.
29. D. Lee, J. Bhardwaj, and J. Jang, based Electrochemical Immunosensor for Label-Free Detection of multiple avian influenza virus antigens using flexible screen-printed Carbon Nanotube-Polydimethylsiloxane Electrodes, *Sci. Rep.*, 2022, **12**(1), p 2311.
30. L. Wang, H. Peng, X. Wang, X. Chen, C. Yang, B. Yang, and J. Liu, PDMS/MWCNT-Based Tactile Sensor Array with Coplanar Electrodes for Crosstalk Suppression, *Microsyst. Nanoeng.*, 2016, **2**(1), p 1-8.
31. O.N. Hur, J.H. Ha, and S.H. Park, Strain-Sensing Properties of Multi-Walled Carbon Nanotube/Polydimethylsiloxane Composites with Different Aspect Ratio and Filler Contents, *Materials*, 2020, **13**(11), p 2431.
32. J. Lu, M. Lu, A. Bermak, and Y.-K. Lee, Study of Piezoresistance Effect of Carbon Nanotube-PDMS Composite Materials for Nanosensors, in 2007 7th IEEE Conference on Nanotechnology (IEEE NANO), (2007) pp. 1240-1243, https://doi.org/10.1109/NANO.2007.4601407
33. N. Mazlan, M. Jaafar, A. Aziz, H. Ismail, and J.J.C. Busfield, Effects of Different Processing Techniques on Multi-Walled Carbon Nanotubes/

Silicone Rubber Nanocomposite on Tensile Strength Properties, in IOP Conference Series: Materials Science and Engineering, vol. 152, no. 1, (2016) p. 012060, IOP Publishing
34. Z. Han and A. Fina, Thermal Conductivity of Carbon Nanotubes and Their Polymer Nanocomposites: A Review, *Prog. Polym. Sci.*, 2011, **36**(7), p 914-944.
35. B.A. Rozenberg and R. Tenne, Polymer-Assisted Fabrication of Nanoparticles and Nanocomposites, *Prog. Polym. Sci.*, 2008, **33**(1), p 40-112.